AIP | Journal of Applied Physics

Er-doped ZnO thin films grown by pulsed-laser deposition

Rafael Pérez-Casero, Araceli Gutiérrez-Llorente, Olivier Pons-Y-Moll, Wilfrid Seiler, Reine Marie Defourneau et al.

Citation: J. Appl. Phys. **97**, 054905 (2005); doi: 10.1063/1.1858058
View online: http://dx.doi.org/10.1063/1.1858058
View Table of Contents: http://jap.aip.org/resource/1/JAPIAU/v97/i5
Published by the American Institute of Physics.

Er-doped ZnO thin films grown by pulsed-laser deposition

Rafael Pérez-Casero,[a] Araceli Gutiérrez-Llorente, and Olivier Pons-Y-Moll
Groupe de Physique des Solides, UMR CNRS 7588, Universités Paris VI et VII, Campus Boucicaut, 140 rue de Lourmel, 75015 Paris, France

Wilfrid Seiler
LM3, ENSAM, UMR CNRS 8006, 151, Boulevard de l'Hôpital, 75013 Paris, France

Reine Marie Defourneau and Daniel Defourneau
Groupe de Physique des Solides, UMR CNRS 7588, Universités Paris VI et VII, Campus Boucicaut, 140 rue de Lourmel, 75015 Paris, France

Eric Millon
LSMCL, Université de Metz, 1, Boulevard Arago, 57078 Metz, Cedex 3, France

Jacques Perrière[b]
Groupe de Physique des Solides, UMR CNRS 7588, Universités Paris VI et VII, Campus Boucicaut, 140 rue de Lourmel, 75015 Paris, France

Philippe Goldner and Bruno Viana
LCAES, ENSCP, UMR CNRS 7544, 11 rue P. et M. Curie, 75321 Paris Cedex 05, France

(Received 21 September 2004; accepted 14 December 2004; published online 11 February 2005)

Crystalline erbium(Er)-doped zinc oxide thin films have been grown by pulsed-laser deposition and were analyzed by the complementary use of Rutherford backscattering spectroscopy, x-ray diffraction analysis, atomic force microscopy, and photoluminescence. The composition, structure, and surface morphology of films were studied, as a function of the growth conditions (temperature from 300 °C to 750 °C and oxygen pressure from 10^{-6} to 0.5 mbar) and Er-doping rate, and were correlated to the emission spectroscopy of Er in the infrared domain. While these studies lead to the determination of optimal conditions for the growth of high crystalline quality films, results of photoluminescence experiments show that the insertion of Er ions in the ZnO matrix does not follow a simple pattern. The Er ions are incorporated from two pathways, one population is found inside the crystallites and another one at the grain boundaries, as a consequence of the differences in valence and ionic radius of Zn and Er. © *2005 American Institute of Physics*.
[DOI: 10.1063/1.1858058]

I. INTRODUCTION

Erbium(Er)-doped semiconductors have attracted interest in optical applications because of the sharp photoluminescence (PL) at 1.54 μm from the intra-4f shell transition in Er^{3+} ions. This emission makes such Er-doped semiconductors suitable candidates for lightwave communication devices such as light-emitting diodes, laser diodes, or planar optical amplifiers.[1] A great deal of work has thus been carried out in the study of the photoluminescence properties of Er-doped low band-gap semiconductors, mainly silicon, in order to enhance the Er-related emission by various means (material annealing, additional oxygen doping).[2,3] Although interesting results have been obtained in the emission intensity at low temperature (77 K), a significant loss in luminescence efficiency occurs at room temperature, precluding their use in practical applications. Indeed, a nonradiative energy backtransfer occurs at room temperature, in which an excited Er ion generates a trapped electron-hole pair.[4] This PL quenching was found to decrease with an increase of the semiconductor band-gap energy,[5] making wide band-gap semiconductors (ZnO, e.g., Eg=3.3 eV) attractive candidates for investigations as hosts for Er doping.

As a result, the optical properties of Er-doped ZnO thin films have been investigated.[6,7] In these studies, the Er-doped ZnO films were grown by pulsed-laser deposition under quite specific experimental conditions (room-temperature deposition followed by a short duration high-temperature thermal treatment) which do not allow to correlate the Er emission properties with the structural and microstructural characteristics of the ZnO host matrix.[6,7] In fact, only the local structure of Er center has been investigated in 0.5% Er-doped ZnO films grown at room temperature followed by a short annealing at 700 °C in oxygen atmosphere.[8] In the as-deposited amorphous films the Er ions are surrounded by five first O atoms and eight O atoms as second nearest neighbors.[8] The short time annealing performed to activate the Er^{3+} ions would change their coordinence, leading to a pseudo octahedral (coordinence 6) local structure resulting in an enhancement of Er-related photoluminescence.[8] Indeed, although the films are heat treated, no detailed information concerning the crystalline state (structure, crystalline quality) of the films is presented.

The growth of crystallized Er-doped oxide thin films has

[a]Permanent address: Departamento de Fisica Aplicada C-XII, Universidad Autonoma de Madrid, 28049 Madrid, Spain.
[b]Author to whom correspondence should be addressed; FAX : 33 01 43 54 28 78; Electronic mail: perriere@gps.jussieu.fr

already been studied in view of planar optical amplifier applications.[9,10] However, the host oxides (Al_2O_3 or Y_2O_3) presented similarities with Er_2O_3 which do not exist in the case of ZnO. Due to the different oxidation state and ionic size of Er^{3+} and Zn^{2+} ions, the insertion of Er in ZnO gives rise to new problems (miscibility of Er in this oxide, lattice distortion, and disorder, …), which could have major effects on the optical emission of Er. Indeed, a photoluminescence quenching appears when the mean distance between two erbium ions is small enough to allow excitation migration and to increase the probability of nonradiative deexcitation.[9] If the Er ions insertion in the ZnO matrix is not complete, the creation of Er-rich zones could allow this concentration quenching, as in the case of Er-doped glasses.

The main purpose of this paper is thus to fill the gap concerning the correlation between the structural and optical properties of Er-doped ZnO films, to enlighten the key parameters that determine their optical quality. We have thus investigated the influence of growth conditions (substrate temperature, oxygen pressure) and Er-doping level of films on their structural and morphological characteristics in order to establish a correlation with their optical properties. The substrates used in this study are (100) silicon wafers covered with 500 nm thick amorphous silica. These SiO_2/Si substrates are known to not favor the growth of epitaxial ZnO films but their low cost and their adaptation to existing microlithography techniques would be two great advantages in the case of a further industrial development in optoelectronics.

II. EXPERIMENT

The undoped and Er-doped ZnO thin films were grown by pulsed-laser deposition onto SiO_2/Si (100) substrates, but for comparison purposes some films were grown on *C*-cut (00.1) sapphire substrates as well. The PLD experimental setup has been described in detail elsewhere.[11,12] Basically, a quadrupled frequency Nd:YAG laser (266 nm) (YAG, yttrium aluminum garnet) is used to ablate the rotating oxide targets. The *in situ* growth of the films was achieved by deposition onto heated substrates (in the 300 °C–750 °C temperature range) under various oxygen pressures (from 10^{-6}–0.5 mbar). After deposition, the films were held at the same temperature during 1 h under a 100 mbar oxygen pressure, and then cooled down to room temperature.

The targets used in this work were sintered pellets of undoped ZnO and Er-doped ZnO with Er concentrations ranging from 0.6–2.8 at. %. The appropriate mixture of ZnO and Er_2O_3 powders was pressed and sintered for 12 h at 1400 °C, in order to obtain hard and compact targets.

The film thickness and composition were determined by Rutherford backscattering spectroscopy (RBS) using the 2 MeV Van de Graaff accelerator facilities of the Groupe de Physique des Solides. The precise concentration and in-depth distribution of the elements were determined by the RUMP simulation software.[13] The films were studied by UV-visible absorption measurements, allowing to evaluate the band-gap value. Microstructure and crystalline orientation of the films were investigated by x-ray diffraction using a Philips X-pert diffractometer with the CuKα radiation ($\lambda \approx 1.54$ Å). The analyses were carried out in the Bragg–Brentano geometry (θ–2θ diagrams) and by rocking curve measurements. The surface morphology of films was studied by a Park scientific instruments atomic force microscope (AFM).

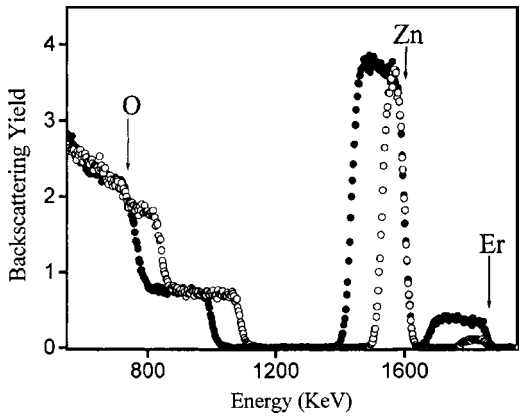

FIG. 1. Rutherford backscattering spectra for 1.5 MeV He^+ ions incident on Er-doped ZnO films grown at 700 °C under 10^{-6} mbar oxygen pressure by pulsed laser ablation of targets whose Er-doping level is 0.6% (hollow circle) and 2% (solid circle), respectively.

The Er-related photoluminescence was analyzed by an ARC SpectroPro 750 monochromator coupled to a N_2 cooled germanium detector. An EG&G 5207 lock-in detection was used for a better noise to signal ratio. Lifetimes were measured under pulsed-laser excitation coming from an OPO (BMI) laser, pomped by the third harmonic of a Nd:YAG laser.

III. RESULTS

A. Film composition

During the high temperature step of the sintering process of doped targets, segregation of the Er species may occur, due to a high diffusivity of Er in the ZnO lattice.[14] Such a phenomenon has been evidenced by RBS analyses of targets, showing an Er enrichment in their near surface region with respect to the bulk concentration. To avoid in-depth heterogeneity in Er content of ZnO films, a careful preablation step (3 h) was systematically carried out before using these targets in thin film growth. With such a process, an in-depth uniform Er concentration was systematically observed in the films, with values equal to those of the target used for the growth (congruence of the PLD process). For instance, Fig. 1 shows typical RBS spectra recorded on films grown on SiO_2/Si substrates by PLD of targets with different Er doping levels. The use of the RUMP simulation program[13] leads to the determination of thickness and composition: 175 nm thick ZnO:Er (2%) and 70 nm thick ZnO:Er (0.6%) films were thus respectively grown, the Er concentration being constant with depth. Moreover, in these spectra, the shapes of the Zn rear edge and Si leading edge of the backscattering contributions indicate that the interface between ZnO and the SiO_2 substrate is quite sharp, and no interfacial reactions (leading to spurious phases) have occurred during the growth process.

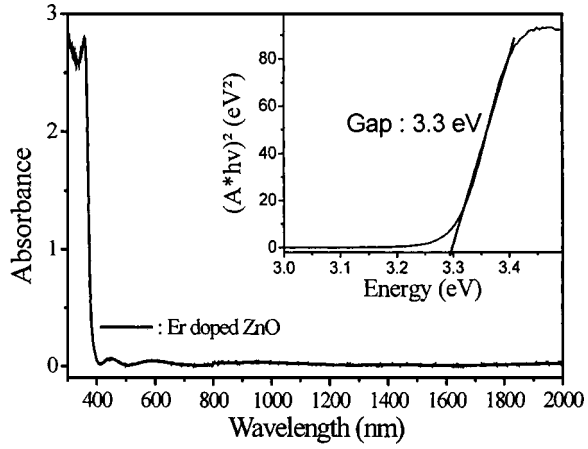

FIG. 2. UV-visible absorption spectrum and corresponding Tauc plot (in insert) for a ZnO:Er (2%) film grown at 700 °C under 10^{-6} mbar oxygen pressure.

Due to the precision of the RBS analysis for the determination of the content in light elements (like oxygen), i.e., about 5%, we cannot exclude a slight oxygen deficiency in the ZnO films. Two reasons can be proposed to explain such a possible deviation in stoichiometry. First, these films are grown under a quite low oxygen pressure that usually involves an unbalanced incorporation of zinc and oxygen atoms into the film. Another reason could be the composition change of the target during laser irradiation. Indeed, it has been reported[15] that the ablated target surface is substantially enriched in Zn, due to backscattering material from the plasma and/or target surface reduction phenomenon.

Oxygen deficiency in ZnO could have important consequences, since oxygen vacancies form defect states in the ZnO band gap which induce shallow traps or a deep-level emission in the visible range, increase the absorption losses and modify the ZnO semiconducting properties. To avoid these consequences, a post growth oxygen annealing step was included in the film formation, in order to compensate the lack of oxygen incorporation during the growth. To check the film stoichiometry, UV-visible absorbance spectra for a doped ZnO film grown on sapphire substrates were recorded and are presented in Fig. 2. A high transmittance ($>90\%$) in the visible region and a sharp absorption edge around 375 nm are observed, without any absorption band above this wavelength. Such films appear thus stoichiometric, since a large amount of defect states associated with oxygen vacancies would lead to a smear absorption edge.[16] Moreover, the absorbance spectrum clearly shows at the absorption edge, the characteristic feature related to the excitonic resonance[17,18] in ZnO, despite the Er doping of the film. From the Tauc plot $[(A h\nu)^2$ as a function of $h\nu]$[19] of the absorption edge region presented in insert, an optical band gap of 3.3 eV can be deduced, a value equal to the one recorded in bulk single crystal ZnO.[20] Finally, the presence of oscillations in Fig. 2, due to interferences in the film, allows to make a rough estimation of the film refractive index. The value found is 2.1, close to the ZnO bulk value. Dark m-lines measurements (carried out at $\lambda = 633$ nm) confirmed that the refractive index is exactly equal to 2, showing that dense ZnO films were obtained.[21]

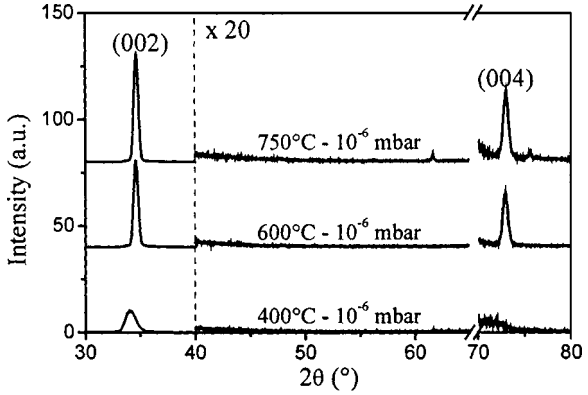

FIG. 3. Normalized x-ray diffraction patterns for ZnO:Er (2%) films grown at various temperature under 10^{-6} mbar oxygen pressure.

B. Film structure and crystalline quality

The influence of the growth conditions on the crystalline state of the films has been studied, and Fig. 3 shows the normalized diffraction patterns (i.e., the diffraction intensities are normalized to the film thickness) of ZnO:Er (2%) films grown under 10^{-6} mbar oxygen pressure at several temperatures. Two well-defined peaks, identified as the (00.2) and (00.4) ZnO diffraction lines, are clearly observed in the diagrams, indicating that the basal planes of the hexagonal ZnO structure are preferentially oriented parallel to the substrate surface. This oriented growth begins to be noticeable at temperatures as low as 300 °C, and is enhanced as temperature increases, as it can be deduced from the evolution of the width and intensity of the corresponding peaks with temperature (Fig. 3).

The influence of the oxygen pressure during the growth was also studied, and Fig. 4 represents the normalized diffraction patterns of ZnO:Er (2%) films grown at 750 °C under several oxygen pressures. An increase in oxygen pressure during the growth leads to a decrease of the diffracted intensity and a slight broadening of the peaks. Moreover, for pressures higher than 0.5 mbar, the preferential (00.1) orientation disappears and the films are polycrystalline.

Finally, the influence of the erbium-doping level has been also studied. Figure 5 presents thus the normalized diffraction patterns of ZnO:Er (x%) films ($x=0$, 2%, and 2.8%) grown at 700 °C under 10^{-6} mbar oxygen pressure.

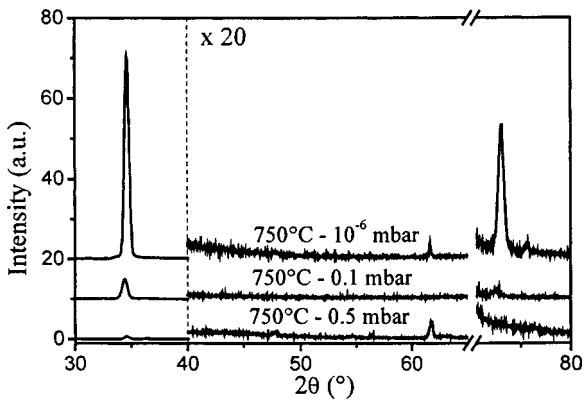

FIG. 4. Normalized x-ray diffraction patterns for ZnO:Er (2%) films grown at 750 °C under various oxygen pressures.

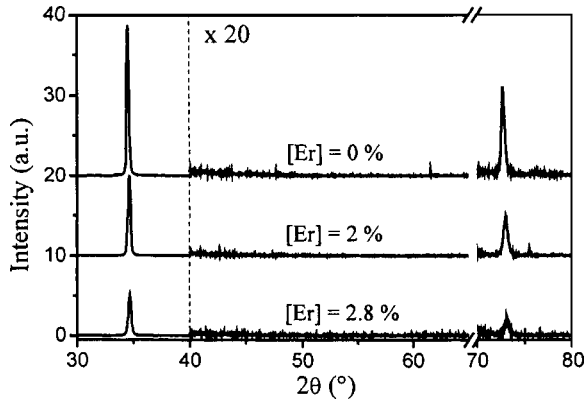

FIG. 5. Normalized x-ray diffraction patterns for ZnO films grown at 700 °C and 10^{-6} mbar with various Er concentrations.

The preferential (00.1) orientation of the films is observed, but the textured growth seems to be favored by low Er-doping levels. In fact, the preferential (00.1) oriented growth is not essentially impeded up to Er levels near to 2%, while higher values lead to a drastic decrease in the intensity of diffraction peaks, meaning that the fraction of crystalline material in the films decreases.

The Bragg angle of the (00.2) and (00.4) peaks allows to determine the *c* parameter of the ZnO cell. Table I presents the evolution of this parameter as a function of growth conditions and Er-doping level. The mean value obtained is comprised between 5.18 and 5.19 Å, which is smaller than the bulk value (5.2066 Å). This can be explained by the fact that films grown by PLD generally present relatively high residual stresses (up to −500 MPa in the case of ZnO (Ref. 22)]. When the temperature decreases, greater values of *c* are obtained, which confirms the crystalline quality degradation at low temperature. In the case of Er-rich films, the *c* parameter tends to decrease. This could be due to the insertion mechanism of Er^{3+} ions in the ZnO würtzite network in which Zn^{2+} ions are in tetrahedral sites. Considering that the doping ions are located on the tetrahedral sites by substitution of the Zn^{2+} ions, the respect of the electrical neutrality of the ZnO crystal imposes the creation of cationic vacancies as the following mechanism:

$$3\ Zn^{2+} \rightarrow 2\ Er^{3+} + V_{Zn^{2+}}.$$

According to the Kröger-Wink notation, this could be written as

$$0 = 2Er_{Zn}^{\cdot} + V_{Zn''}$$

The induced cationic vacancies created by Er doping could therefore induce a shrinking of the network, and consequently a decrease of the unit cell parameters.

Whatever the growth conditions and the Er concentration, the films present a preferred *c*-axis orientation. The existence of a texture in thin film growth is classically explained by surface free energy considerations, the films growing with an orientation minimizing this energy, i.e., in general, the planes with the lowest surface energy are found parallel to the substrate. The case of ZnO is somewhat different because the (00.1) planes do not correspond to a minimum in free surface energy. On the contrary, due to the würtzite structure, consisting in interpenetrating O and Zn hexagonal close packed lattices, the crystal in the *c* direction is an alternate stacking of pure oxygen planes and pure zinc ones. These (00.1) planes are thus charged and their free surface energy diverges,[23] while the prismatic planes [such as (10.0)] are nonpolar and thus have a finite surface energy. This results in a columnar growth, limiting the (00.1) planes area to the top of growth islets, which has been observed in ZnO films synthesized by PLD and other methods.

In addition, pole figures of the (11.1) ZnO planes were recorded, and showed a fiber texture without any in-plane preferential orientation. This fiber texture could be expected since the amorphous nature of the SiO_2 layer does not provide any oriented pattern to lead the in-plane orientation of the growing film.

Rocking curve measurements through the full width at half maximum (FWHM) of the diffraction peaks provide information on the mosaic spread of the films, i.e., on the grain

TABLE I. *c* parameter calculated from the (00.2) peak position, Rocking Curve FWHM, and rms roughness of ZnO films grown under various conditions of temperature, pressure, and Er-doping rate. Two samples with the same deposition conditions (labeled *) are presented in order to get an estimation of the precision of the experimental results.

Temperature (°C)	Oxygen pressure (mbar)	Er doping rate at. %	*c* parameter (Å)	Rocking curve FWHM (deg)	rms roughness (nm)
400	10^{-6}	2.0	5.266	4.7	0.8
500	10^{-6}	2.0	5.250	2.8	3.3
600	10^{-6}	2.0	5.184	2.3	3.2
700*	10^{-6}	2.0	5.181	2.1	3.2
750	10^{-6}	2.0	5.181	2.1	3.8
750	10^{-2}	2.0	5.210	7	8.8
750	0.5	2.0	5.188	···	26.7
700	10^{-6}	0.0	5.191	1.3	3.5
700	10^{-6}	0.6	5.203	2.1	3.2
700*	10^{-6}	2.0	5.187	2.2	3.2
700	10^{-6}	2.8	5.169	3.0	5.0

disorientation. Table I shows the evolution of the FWHM of the ZnO (00.2) diffraction peak as a function of the growth parameters and Er-doping rate. First, the crystalline quality tends to rapidly improve with temperature up to 600 °C, while it hardly changes as temperature increases further. Thus, 600 °C appears as a minimum threshold value to grow films of good crystalline quality even if ZnO crystallization and oriented growth take place at lower temperatures. The rather large FWHM values observed in this work (2.1°) even for films grown at 750 °C under 10^{-6} mbar is related to the amorphous nature of the SiO_2 substrate used for the growth, and is identical to the best values reported for ZnO growth on amorphous substrates.[24] The FWHM values are roughly constant up to a pressure of 10^{-3} mbar, which proves that the degree of disorientation of the ZnO (00.1) planes is not modified in the 10^{-6}–10^{-3} mbar range. Beyond this value, the higher the pressure, the worse the crystalline quality of the film. As a result, largely disordered films are grown under 0.5 mbar oxygen pressure.

The decrease in crystalline quality with an increase of the oxygen pressure has to be related to the decrease of the kinetic energy of species reaching the growing film surface. In the literature, ZnO films with the best crystalline quality (in terms of lowest values of FWHM of rocking curves) were obtained around 700 °C–750 °C under a wide range of oxygen pressure, from 10^{-5} Torr (1.3×10^{-5} mbar) up to 10 mTorr (1.3×10^{-2} mbar).[25] Indeed, these optimized growth conditions are related to the target-to-substrate distance d which differs in the various studies. The oxygen pressure P and the distance d are linked through the following relationship: $P\times d^{\gamma}=$constant (γ being comprised between 2 and 3) which determines the optimum growth conditions.[26] Thus, any variation of the distance d will induce a correlated variation in the optimal oxygen pressure. The value of pressure found in this work (10^{-6}–10^{-3} mbar) is in very good agreement with the values reported for the growth of ZnO films on silica substrates[24] with a comparable geometry, which shows a drastic increase in the FWHM of rocking curve when the oxygen pressure is higher than 10^{-3} mbar.

The FWHM value strongly varies with the Er-doping level (Table I). An increase of the FWHM value with an increasing Er content is observed, indicating the clear deleterious effect of Er incorporation in the lattice on ZnO crystalline quality. This effect occurs even at small doping levels, since the FWHM value of ZnO:Er (0.6%) films is almost twice the one of pure ZnO films. Nevertheless, the results also indicate that the oxide structure can admit some degree of doping without further increase in the disorientation of the crystallites, as it is reflected by the fact that the FWHM value hardly changes when the doping rate ranges from 0.6% to 2%. This latter value would be roughly the maximum admissible doping level without larger degradation of the oriented growth, since larger FWHM values are obtained for doping levels higher than 2%.

C. Surface morphology

Atomic force microscopy has been used to study the surface morphology of the ZnO films, and Table I shows the values of the root mean square (rms) surface roughness of ZnO:Er films for different substrate temperatures, oxygen pressure, and Er-doping levels. The corresponding AFM images are presented in Fig. 6, and may be correlated to the previously studied structural characteristics. At low temperatures ($T<300$ °C), amorphous films are formed and the AFM image does not show any particular structure and exhibits a low surface roughness (0.8–0.9 nm). As temperature increases, ZnO film crystallization occurs and the AFM image of the film grown at 500 °C shows a granular structure, with a low surface roughness (3 nm). This can correspond to the columnar structure which is associated with the (00.1) ZnO textured growth. Further increase in temperature (700 °C) does not seem to involve large evolution of neither the structure nor the film surface roughness.

The mean surface roughness of films increases by almost one order of magnitude when the oxygen pressure changes from 10^{-6} to 0.5 mbar. However, this increase is not linear. In fact, the mean roughness remains constant around 3 nm for pressures from 10^{-6} up to 10^{-2} mbar. Then, the surface structure dramatically evolves with the oxygen pressure as it is shown in the images in Fig. 6. The grains observed in the surface of the films grown at 10^{-6} mbar become large coarsened droplets at 0.5 mbar.

The study of the influence of the Er-doping level on the surface morphology shows that slightly doped films ([Er] $=0.6$ at. %) exhibit low mean roughness values around 1 nm. The surface roughness increases as the erbium rate increases, leading to non-negligible values of 5 nm for largely doped films ([Er]$=2.8$ at. %).

D. Optical properties

The Er-emission properties were studied as a function of the growth parameters and the Er-doping level, in order to correlate the photoluminescence characteristics to the structural features of the films. However, the results obtained were unexpected. Figure 7 compares spectra obtained for a ZnO:Er (2%) film and an Y_2O_3:Er (5%) film, both grown at 700 °C under 10^{-6} mbar. The emission in the yttria film presents clear Stark sublevels transitions.[21] Since both films, obtained in the same growth conditions, exhibit a good crystalline quality, a similar emission was expected. But the ZnO film emission is broad, with a maximum at 1.535 μm, two large shoulders at 1.546 and 1.557 μm, and without any Stark sublevels structure. This emission shape is usually observed in amorphous materials, such as glass films.[9] Moreover, the emission is about 500 times less intense than in the case of the Y_2O_3 film, for a similar film thickness.

This broad emission depends on the growth conditions and Er-doping level. First, Figs. 8 and 9 show a clear decrease of the emission intensity with a decrease of the temperature or an increase of the oxygen pressure. A similar behavior is observed for the diffraction peak intensity (Figs. 3 and 4). Furthermore, Fig. 10 exhibits a concentration quenching, since the emission intensity peaks for a 2% doping, and then drastically decreases.

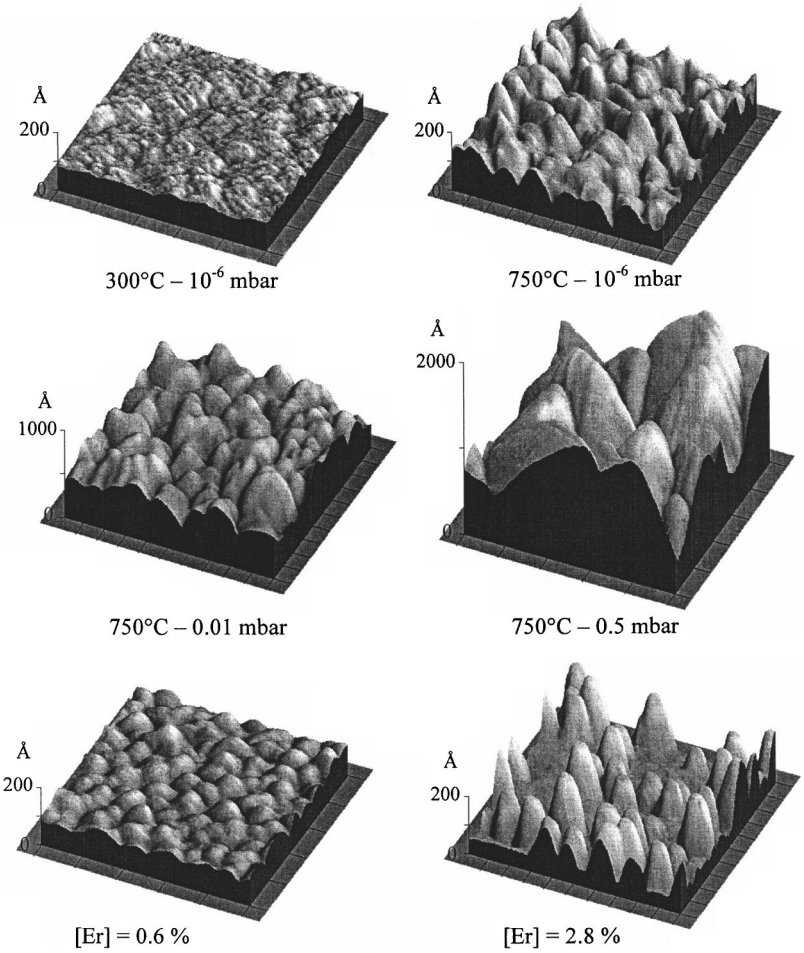

FIG. 6. Evolution of the AFM images with the temperature, the pressure, and the Er-doping rate.

IV. DISCUSSION

These PL features should be commented and compared to the structural characteristics of the films, in order to show that the insertion of Er ions in ZnO films is not a simple issue. First, the emission shape, identical to the one observed in amorphous materials, seems to evidence that the Er ions are not surrounded by a well-ordered environment. Moreover, the emission intensity drastically decreases in Er-rich films. These results strongly suggest that the Er ions could be present outside the crystallized ZnO grains, i.e., in grain boundaries as it has been observed in bulk materials.[27,28]

However, we have shown that the *c* parameter of the ZnO cell, the crystalline quality and the surface morphology are linked to the Er content. This means that the Er ions play a role in the crystallization process and that a part of these Er ions is present inside the crystallized grains. This is also consistent with the fact that the photoluminescence intensity depends on the growth temperature and pressure (Figs. 8 and 9). If the Er ions were all located outside the grains, the PL

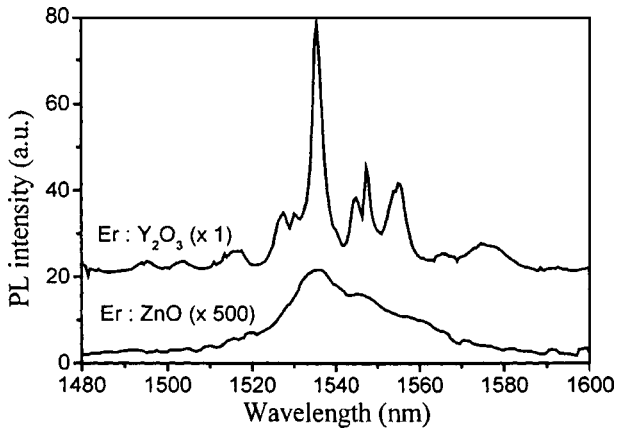

FIG. 7. Photoluminescence spectra of Er-doped Y_2O_3 and ZnO films grown in similar conditions, (700 °C and 10^{-6} mbar).

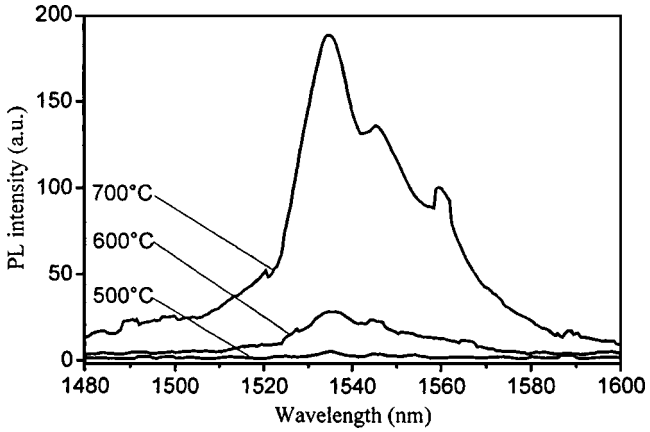

FIG. 8. Evolution of the PL spectrum of ZnO:Er (2%) films grown at various temperatures under 10^{-6} mbar oxygen pressure.

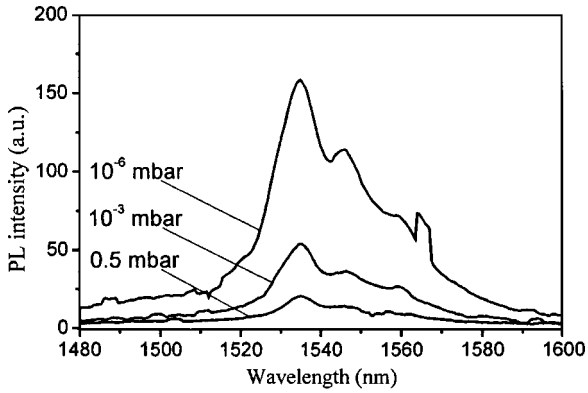

FIG. 9. Evolution of the PL spectrum of ZnO:Er (2%) films grown at 750 °C under various oxygen pressures.

intensity should not depend on the growth conditions. The presence of Er ions inside the ZnO grains is also confirmed by Williamson–Hall analysis,[29] linking the width and the Bragg angle of the (00.2) and (00.4) peaks, from which strain values (ε) can be evaluated. In the case of pure ZnO films, these strains are equal to -0.7×10^{-3}. But, when the Er concentration is increased, higher strains are observed, reaching 7.5×10^{-3} for ZnO:Er (2.8%) films. This means that at least a fraction of the Er ions is present in the ZnO crystallites and that these ions induce important strains in the ZnO matrix. These strains observed in the doped films could create a local disorder around the Er ions, which could partly explain the broad emission obtained at 1.5 μm.

There are thus experimental evidences proving that the Er ions are both inside and outside the ZnO grains. These contradicting results raise the issue of the exact location of the Er ions in the ZnO films.

A complete substitution of the Zn ions can be obtained by Er ion implantation.[14,30] In that case, up to an Er-doping rate of 0.665%, it has been showed that the Er ions are inserted in a position very close to the Zn crystallographic site situated at 0.25 Å above the Zn site along the *c* axis. Nevertheless, in such doping method, the Er ions are in a nonequilibrium state. When the implanted films are heat treated at temperatures higher than 700 °C, a diffusion of most of the Er ions towards the surface is obtained.[14,30] Thus, whatever the doping process, segregation of the Er ions outside the grains is often observed.

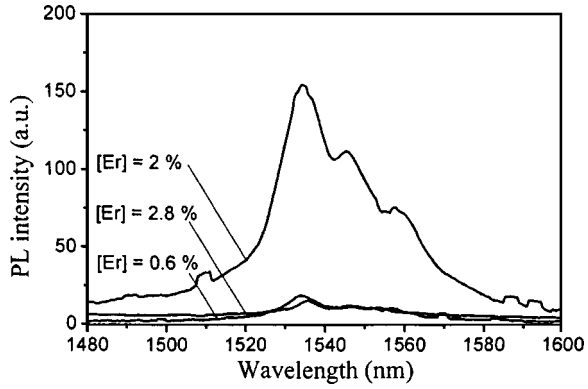

FIG. 10. Evolution of the PL spectrum of ZnO:Er (2%) films grown at 700 °C and 10^{-6} mbar oxygen pressure, with various Er concentrations.

As mentioned previously, the difference in the respective valence of Er (3) and Zn (2), and ionic radii (0.89 Å for Er^{3+} in coordinence 6, and 0.60 Å for Zn^{2+} in coordinence 4) can be a problem for the insertion of Er in the hexagonal würtzite lattice of zinc oxide. Doping ions are frequently added to zinc oxide to modify or enhance some of its physical properties.[31] Though the precise mechanism of rare earth (RE) doping is not well known, the incorporation mechanisms of such elements in the würtzite network appear limited. The first one consists in the insertion of RE ions in the nonoccupied positions of the ZnO structure: four sites in coordinence 6 per unit cell are possible and the maximum radius of these unoccupied crystallographic positions is 0.88 Å, which is the theoretical ion size upper limit allowed. Nevertheless it has never been demonstrated that ions with an important size (such Er^{3+}) follow this insertion pathway. It has even been shown that Zr^{4+} (0.59 Å in coordinence 4), which is smaller than Zn^{2+}, cannot occupy the interstitial position in the ZnO network, and should prefer to agglomerate at the grain boundaries.[32] As it has been reported for the doping by small size elements (i.e., Ti^{4+}) in ZnO films,[33] the second possibility is the substitution of the Zn^{2+} ions in the lattice but the only experimental result highlighting such a mechanism with large ions like Er^{3+} is obtained by ion implantation,[14,30] which does not lead to the same incorporation process than for the deposition methods (see above). Finally, as it has been proposed for ZnO bulk ceramics,[27,28] one may consider that the large size trivalent rare earth ions acts as grain growth inhibitors, and should prefer to aggregate at the grain boundaries. This segregation in the grain boundaries would explain the amorphouslike emission, the dramatic decrease of the emission intensity for the highest Er-doping rate and also the relative low Er emission in all the films, compared to other crystallized films. This low emission made $^4I_{13/2}$ level lifetime measurements impossible with our setup, while this feature would be essential to know if the Er ions have segregated. Indeed, in Er-rich regions, this $^4I_{13/2}$ level lifetime would be short (a few tens of microsecond) due to Er–Er interactions. The observed emission could thus be due to both Er ions located in the ZnO matrix and Er ions segregated at grain boundaries.

Our PL results are also quite different from the ones obtained on PLD films grown at ambient temperature and heat treated after deposition.[6,7] These last films exhibit an Er emission somewhat intermediate between the one observed in Fig. 7 for Er-doped Y_2O_3 and ZnO films with a long $^4I_{13/2}$ lifetime (2 ms). In that case, the amorphous films are heat treated for a short time (5 min) at 700 °C before any PL measurement, as in the case of glass films. This thermal treatment used to "activate" the Er ions, could allow a reorganization of the oxygen ions around the Er ions, leading to a better Er emission at 1.5 μm, while being too short to observe any Er segregation as in our films.[8] These growth conditions being quite different from the ones used in this study, it is uneasy to compare these results, but our PL and structural features tend to prove that two different Er populations are present in our films, one inside the crystallized grains and another in the grain boundaries. Furthermore, even if our films present diffraction features of crystallized

ZnO films, other results prove that strains exist in the crystallites, which could broaden the Er emission.

V. CONCLUSION

We present in this work a complete study of the evolution of the crystalline state and surface morphology of PLD grown Er-doped ZnO films, as a function of the growth parameters and the doping rate. While this study leads to the determination of optimal conditions (high temperature and low pressure) for the growth of dense, good crystalline quality and relatively smooth films, the PL experiments show that the insertion of the Er ions in the ZnO matrix does not follow a simple pattern and that the Er ions are probably not only located inside the crystallized grains but also at the grain boundaries, leading to strong luminescent quenching.

This makes the understanding of the PL features and the optimization of the Er emission difficult. In future, an interesting approach could be the study of doped films epitaxied on substrates such as sapphire, for example. Indeed, it has been shown that in the case of ZnO films epitaxied on *c*-cut sapphire, doping rates as high as 30% can be incorporated, for Co^{2+} and Mn^{2+} or Mg^{2+} ions, without any segregation.[31,34] Even if the valence of Er is different from the Zn one, a similar stabilization by epitaxy could lead to a minimization of the Er segregation outside the grains and then to a stronger Er emission at 1.5 μm

ACKNOWLEDGMENT

R.P. was supported by the Ministrerio de Ciencia y Technologica of Spain (Grant No. HF-2001-0045).

[1]T. Gregorkiewicz and J. M. Langer, MRS Bull. **24**, 27 (1999).
[2]K. Takahei and A. Tagushi, J. Appl. Phys. **74**, 1979 (1993).
[3]H. Efeoglu *et al.*, Semicond. Sci. Technol. **8**, 236 (1993).
[4]P. G. Kik, Ph.D. thesis, University of Utrecht, Utrecht, Netherlands.
[5]P. N. Favennec, H. L'Haridon, M. Salvi, D. Moutonnet, and T. Le Guillou, Electron. Lett. **25**, 718 (1989).
[6]S. Komuro, T. Katsumata, T. Morikawa, X. Zhao, H. Isshiki, and Y. Aoyagi, Appl. Phys. Lett. **74**, 377 (1999).
[7]S. Komuro, T. Katsumata, T. Morikawa, X. Zhao, H. Isshiki, and Y. Aoyagi, J. Appl. Phys. **88**, 7129 (2000).
[8]M. Ischii, S. Komuro, T. Morikawa, and J. Aoyagi, J. Appl. Phys. **89**, 3679 (2001).
[9]A. Polman, J. Appl. Phys. **82**, 1 (1997).
[10]O. Pons-Y-Moll *et al.*, J. Appl. Phys. **92**, 4885 (2002).
[11]P. H. Haumesser, J. Thery, P. Y. Daniel, A. Laurent, J. Perrière, R. Gomez-San Roman, and R. Perez-Casero, J. Mater. Chem. **7**, 1763 (1997).
[12]A. Huignard, A. Aron, P. Aschehoug, B. Viana, J. Thery, A. Laurent, and J. Perrière, J. Mater. Chem. **10**, 549 (2000).
[13]R. L. Doolittle, Nucl. Instrum. Methods Phys. Res. B **9**, 344 (1985).
[14]The ISOLDE Collaboration, U. Wahl, E. Rita, J. G. Correla, E. Alves, and J. P. Aranjo, Appl. Phys. Lett. **82**, 1173 (2003).
[15]F. Claeyssens, A. Cheesman, S. J. Henley, and M. N. R. Ashfold, J. Appl. Phys. **92**, 6886 (2002).
[16]J. Yin, Z. G. Liu, H. Liu, X. S. Wang, T. Zhu, and J. M. Liu, J. Cryst. Growth **220**, 281 (2000).
[17]A. K. Sharma, J. Narayan, J. F. Muth, C. W. Teng, C. Jin, A. Kvit, R. M. Kolbias, and O. W. Holland, Appl. Phys. Lett. **75**, 3327 (1999).
[18]C. W. Teng, J. F. Muth, Ü. Özgur, M. J. Bergmann, H. O. Hewitt, A. K. Sharma, C. Jin, and J. Narayan, Appl. Phys. Lett. **76**, 979 (2000).
[19]*Optical Properties of Solids*, edited by J. Tauc and F. Abeles (North Holland, Amsterdam, 1971), p. 277.
[20]D. E. Gray, *American Institute of Physics Handbook*, 3rd ed., (AIP, New York, 1972), pp. 9–24.
[21]O. Pons Y Moll, Ph.D. thesis, Université Paris 6, Paris, France.
[22]J. Perrière, E. Millon, W. Seiler, C. Boulmer-Leborgne, V. Craciun, O. Albert, J. C. Loulergue, and J. Etchepare, J. Appl. Phys. **91**, 690 (2002).
[23]P. W. Tasker, J. Phys. C **12**, 4977 (1979).
[24]S. Masuda, K. Kitamura, Y. Okumora, S. Myatake, H. Tabata, and T. Kawai, J. Appl. Phys. **93**, 1624 (2002).
[25]S. Choopun, R. D. Vispute, W. Noch, A. Balsamo, R. P. Sharama, T. Venkatesan, A. Lliadis, and D. C. Lock, Appl. Phys. Lett. **75**, 3947 (1999).
[26]H. S. Kwok, H. S. Kim, D. H. Kim, W. P. Shen, X. W. Sun, and R. F. Xiao, Appl. Surf. Sci. **109-110**, 595 (1997).
[27]S. Bachir, K. Azuma, J. Kossanyi, P. Valat, and J. C. Roufart-Haret, J. Lumin. **75**, 35 (1997).
[28]J. C. Ronfart-Haret, and J. Kossanyi, Chem. Phys. **241**, 339 (1999).
[29]B. H. Hwang, and S. Y. Chiou, Thin Solid Films **304**, 286 (1997).
[30]E. Alves, E. Rita, U. Wahl, J. G. Correia, T. Monteiro, J. Soares, and C. Boemare, Nucl. Instrum. Methods Phys. Res. B **206**, 1047 (2003).
[31]Z. Jin, M. Murakami, T. Fukumura, Y. Matsumoto, A. Ohtomo, M. Kawasaki, and H. Koinuma, J. Cryst. Growth **214-215**, 55 (2000).
[32]G. K. Paul, S. Bandyopadhyay, S. K. Sen, and S. Sen, Mater. Chem. Phys. **79**, 71 (2003).
[33]Y. M. Lu, C. M. Chang, S. I. Tsai, and T. S. Wey, Thin Solid Films **447-448**, 56 (2004).
[34]W. Yang, S. S. Hullavarad, B. Nagaraj, I. Takeushi, R. P. Sharma, T. Venkatesan, R. D. Vispute, and H. Shen, Appl. Phys. Lett. **82**, 3424 (2003).